SCALE-MODEL EVALUATION OF FRICTIONAL EFFECTS AND REDIRECTION MECHANISMS FOR ANGLE BARRIER IMPACTS

Brent R. Helm, Joseph C. Free, Charles Y. Warner, and Greg B. Frandsen,
Department of Mechanical Engineering,
Brigham Young University and Eyring Research Institute

The effects of friction at the car-barrier interface in angular collisions have been investigated by using a 1/24 scale model. Results demonstrate that interface friction can have a great effect on both vehicle trajectory and predicted damage to car and barrier. Friction thresholds for successful redirection are related to vehicle and barrier stiffness, impact angle, and impact speed, but low-friction values show promise of improving accidental barrier impacts at all speeds and angles tested.

•WHEN an automobile collides with a guardrail or gore barrier at 60 mph (96.6 km/h) and 25 deg, seemingly insignificant design details can have tremendous effects on the outcome. The snagging of the vehicle on guardrail or barrier should probably be avoided more than any other peril except penetration through the barrier. (In some installations penetration is possibly less dangerous than snagging.) The influence of the tangential force in the barrier (Figure 1) is significant in the overall vehicle dynamics of such an impact, since it introduces an unstable moment on the vehicle which, if not counteracted, leads to snagging or, at best, dangerous trajectories.

The importance of friction, as defined here, has been acknowledged in the development of traffic barriers. The use of the blockout and rub rails on the MB4 median barrier was recommended to avoid the frictional force of snagging vehicle tires against barrier posts (4, 5). However, this is not the kind of friction that can be easily handled by lubrication. Successful design must provide good force-distribution structures, to limit local stresses at sliding interfaces to reasonable levels. When this is done, lubrication methods can be considered for improvements.

In actual practice, the dynamic interfacial effects are somewhat more imposing than those normally connoted by the term friction. They can range all the way from paint scraping to shearing off a complete front wheel and suspension. Management of these forces in practice is complicated by diverse geometry in vehicle and barrier design, by the wide diversity in significant vehicle dynamic characteristics, and by the more subtle nondesign that results in more or less random load paths within automobile bodies of different makes and models. The advent of federal motor safety standards may be expected to reduce the broad scatter of automobile crash dynamics somewhat with stiffer bumpers already on the street (1) and stiffer substructure to come (2, 3).

Figure 2 shows an example, from scale-model testing, of the catastrophic redirectional trajectory that is a result of high friction. The objective of this paper is to demonstrate that proper management of interfacial friction can have tremendous effect on the severity of a side-angle impact and to identify rough guidelines for improvement in barrier design.

SCALING LAWS AND MODEL PARAMETERS

The scale-modeling procedure has previously been applied successfully to complex dynamic impact situations (6, 15). Given the complex interactions of the angle barrier crash, it is perhaps the best single technique for engineering insight at low cost.

In their development of a planar, rigid-car model for frontal impact attenuator

Figure 1. Idealized forces in horizontal place, car-barrier angle impact.

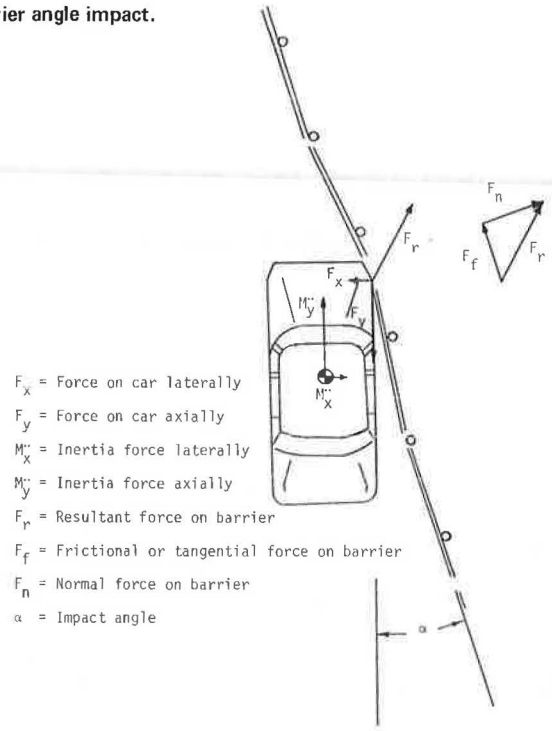

Figure 2. Trajectory at 58 mph (93.3 km/h) and 25 deg as a result of high friction.

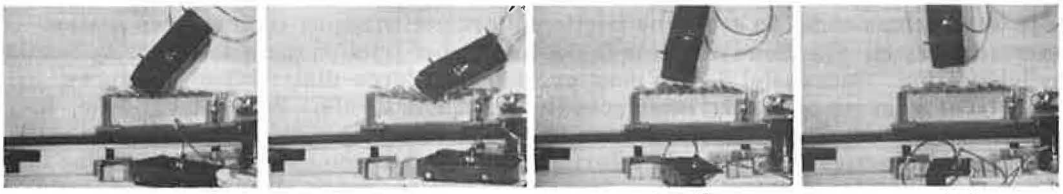

Figure 3. Model-vehicle body and chassis.

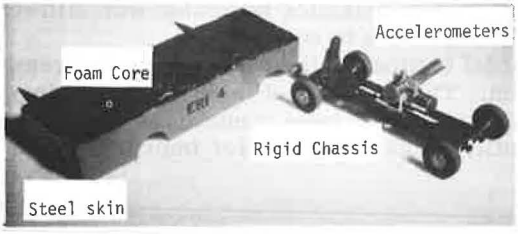

Figure 4. Measurement of vehicle crush.

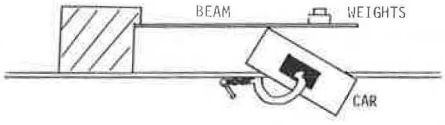

crashes, Fay and Wittrock (9) have developed appropriate scaling laws from dimensional analysis. This process was extended in the present study to include a representation of vehicle deformation by using the frontal crash characteristics [linear ramp; slope of 12 *g*/ft (12 *g*/m)] recommended by Emori (10). The model was then constructed with a solid core enclosed in a viscoelastic foam body with a 0.004-in. (0.01-cm) steel skin (Figure 3). For experimental convenience, the length scale was $\frac{1}{24}$, and the acceleration scale was set equal to one. From these two selections, the time scale was calculated. The mass scale was selected to match barrier cable force and deflection. The static force-deflection behavior of the model was measured as shown in Figure 4. The resulting force-deflection curves are shown in Figure 5.

Since the phenomena under investigation are expected to be largely two dimensional, the pitch and yaw moments of inertia were deemed to be quite important. These were scaled to prototype equivalents by weighing the rigid core of the vehicle and by proper accelerometer placement. Mass moments of inertia of model roll, pitch, and yaw were determined by calibrating a torsional pendulum with a rod of known moment of inertia and then by suspending the car at the center of gravity along each axis and measuring the natural frequency of the car. The mass moment of inertia was obtained by using the equation:

$$I = \frac{K}{\omega^2} \tag{1}$$

where

I = mass moment of inertia in slug-inch^2 (kilogram · meter^2),
K = torsional spring constant in pound-force-inch/radian (newton · meter/radian), and
ω = natural frequency in radians/sec.

A summary of the scaling factors used is given in Table 1.

Table 2 gives scaled parameters for the car and barrier with the maximum scaling error. The large error in wheel weight of the vehicle was not considered significant because its rotational energy was less than 6 percent of the total vehicle energy.

Verification of the model car was done by a scale-model simulation, similar to the profile developed by New Jersey (18), of actual full-scale impacts of the type 50 prestressed concrete median barrier. Figure 6 correlates the longitudinal and lateral acceleration traces for the model and the full-sized vehicle for an impact at 25 deg and 60 mph (96.5 km/h). The plots are in general agreement.

Model vehicle and barrier surfaces were matched in the following ways to obtain a range of friction coefficients:

1. For low friction, a clear plastic cover was placed over the fish scales with a lightweight bearing oil sandwiched between, and a painted surface was used on the car body. The resulting static coefficient of friction was about 0.1.
2. For medium friction, surfaces were painted on the fish scales, and a surface was painted on the car body. The resulting static coefficient of friction was about 0.85.
3. For friction, medium-grade sandpaper squares were glued to fish scales, and the car body was covered with silicone rubber. The resulting static coefficient of friction was about 1.35.

The coefficients of friction were determined by placing the proper surfaces together, by using a known weight to produce a lateral force F, and by using another known weight to produce a normal force N.

When the correct forces F and N were applied so that the frictional surfaces were just on the verge of slippage, the coefficient of friction was calculated by using the equation,

Figure 5. Force-deflection curve for model-vehicle crush.

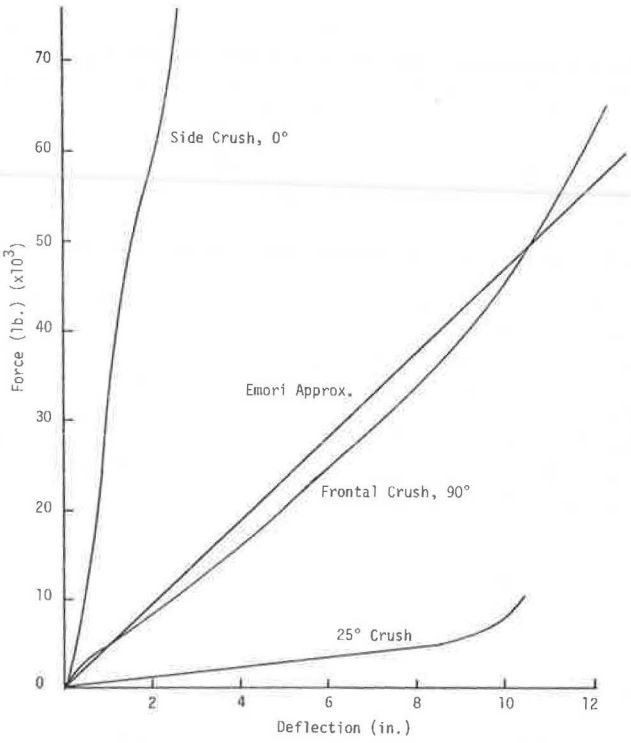

Table 1. Scaling factors.

Item	Measurement
Length	$\frac{1}{24}$
Time	$(\frac{1}{24})^{0.5} = 0.204$
Mass	8.0295×10^{-5}
Acceleration	1
Velocity	0.204
Force	8.0295×10^{-5}
Mass moment of inertia	1.394×10^{-7}
Force versus deflection	1.927×10^{-3}

Table 2. Vehicle and barrier parameter scaling.

Parameter	Prototype	Model	Maximum Error (percent)
Vehicle weight, lb	4,700	0.377	5
Track width, in.	70	2.9	5
Wheel base, in.	120	5	5
Roll, lbf-in.-sec^2	4,989	0.0006958	1
Pitch, lbf-in.-sec^2	25,641	0.00379	1
Yaw, lbf-in.-sec^2	34,335	0.003942	4
Frontal crush, lbf/ft	56,400	144.9	10

Note: 1 lb = 0.45 kg. 1 in. = 2.54 cm. 1 lbf-in.-sec^2 = 11.29 N-cm-s^2. 1 lbf/ft = 14.6 N/m.

Figure 6. Verification of model test results.

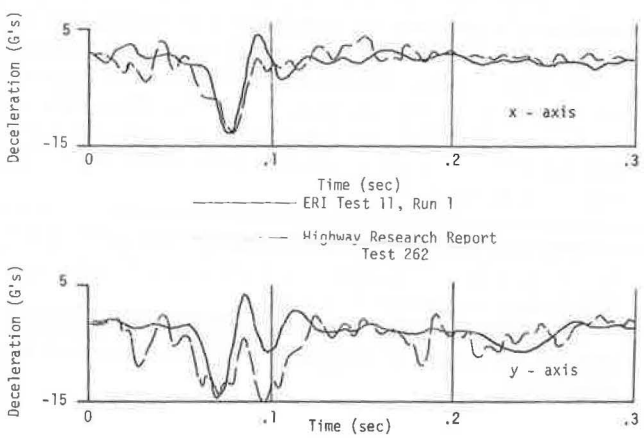

$$\mu = F/N \quad (2)$$

TEST PROCEDURE

Tests were conducted on a 5 by 9-ft (1.5 by 2.7-m) table. The model vehicle was accelerated to impact velocity by a tow cable passed around guide pulleys and into a network of multiplying pulleys attached to a weight (Figure 7). The weight was held suspended until the beginning of the test and then was released by an electric solenoid. A cable trailing the vehicle released the tow cable just before impact. The vehicle velocity was determined by recording the time interval between electrical impulses generated by two metal bands on the tow cable that were positioned to pass an electromagnetic pulse generator just before the tow cable was released.

Vehicle accelerations were obtained by two piezoelectric accelerometers mounted at the vehicle's center of gravity. Low noise data lines were trailed behind the vehicle.

Barrier cable loads were obtained from a piezoelectric load cell mounted in the barrier. Data from the piezoelectric transducers were amplified by charge amplifiers. Velocity-time impulses and amplified transducer data were recorded simultaneously on a four-trace oscilloscope picture and on a computer data acquisition system that uses a minicomputer to record the data through an analog-to-digital converter.

The data were scaled and digitally filtered through a fourth-order Butterworth filter with a cutoff frequency of 200 Hz and were plotted by the digital data acquisition system. Data were from high-speed movie film shot at 500 frames/sec. A mirror system was used to obtain simultaneous top and side views.

TEST RESULTS

Figures 2, 8, and 9 show the details of the vehicle-barrier interaction for situations of high, medium, and low friction.

Figure 10 shows the catastrophic behavior as a result of high friction when the vehicle exits at about 90 deg into parallel traffic lanes. The comparison in Figure 10 shows that the barrier cable forces resulting from high friction were approximately 1.5 times those resulting from medium friction and 2.0 times those resulting from low friction. These higher forces have implications for actual barrier designs since they would induce further failure of a barrier structure. It appears that, if the force on the vehicle parallel to the barrier is high enough to induce an angular velocity (CCW in this case), no recovery is possible. The higher forces thus generated cause a moment that increases the angular velocity.

Although the high-speed film data of Figures 8 and 9 show a similar qualitative behavior for medium and low friction, the comparison of deceleration rates as shown in Figure 11 shows that axial decelerations for low friction were less than 50 percent of those for medium friction. These reductions in deceleration imply that for actual crash situations vehicle crush and front wheel damage in low-friction situations would be reduced, damage repair costs would be reduced, and postcrash maneuverability would be improved.

Average pulse decelerations for three runs each at medium and low friction are given in Table 3. The axial decelerations are consistently lower for low friction, and the average of the lateral decelerations is 20 percent higher for low friction. However, these high lateral loads occur during the secondary lateral impact of the side and rear of the vehicle and are thus unlikely to cause significant damage or deviant trajectories. The time shift of the axial pulse and the lateral pulse is shown in Figure 11.

CONCLUSIONS

For the scaled velocities tested and a cable-plate type of redirecting system interacting with a scaled 4,700-lb (2130-kg) vehicle of the stiffness profile shown in Figure 5, the

Figure 7. Scale-model test facility.

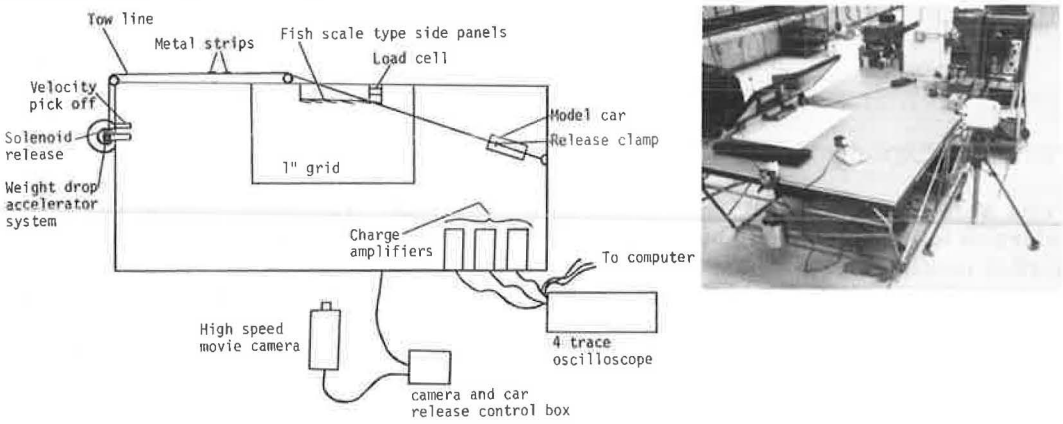

Figure 8. Trajectory at 61 mph (98.2 km/h) and 25 deg as a result of medium friction.

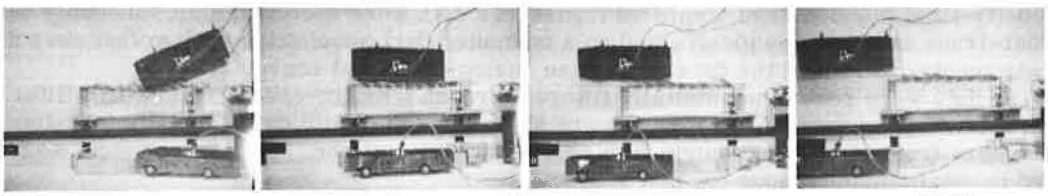

Figure 9. Trajectory at 61 mph (98.2 km/h) and 25 deg as a result of low friction.

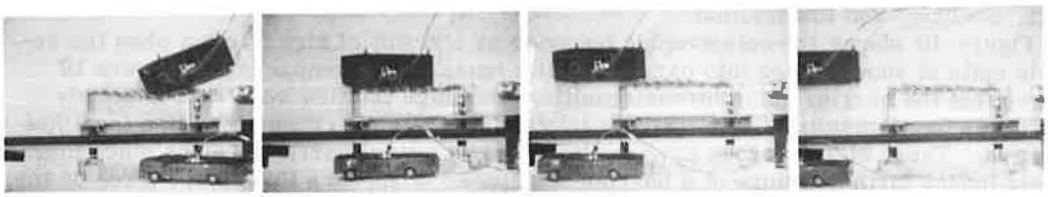

Figure 10. Barrier load versus time.

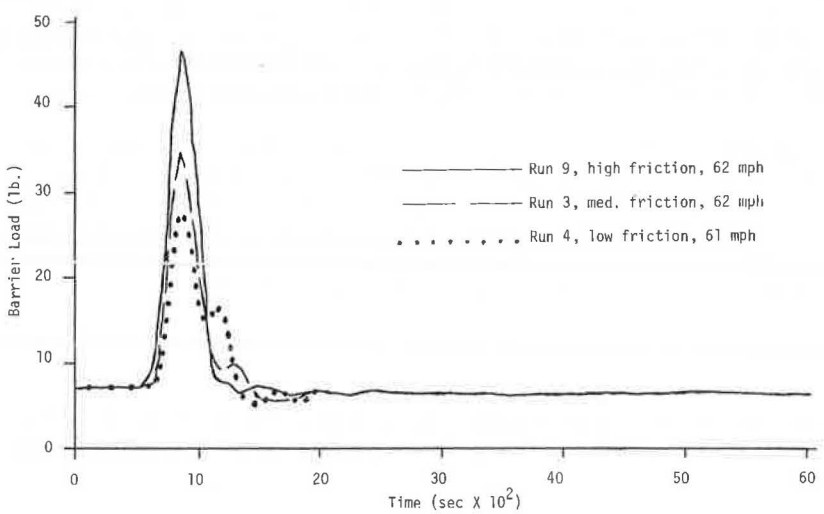

Figure 11. Deceleration rate versus time.

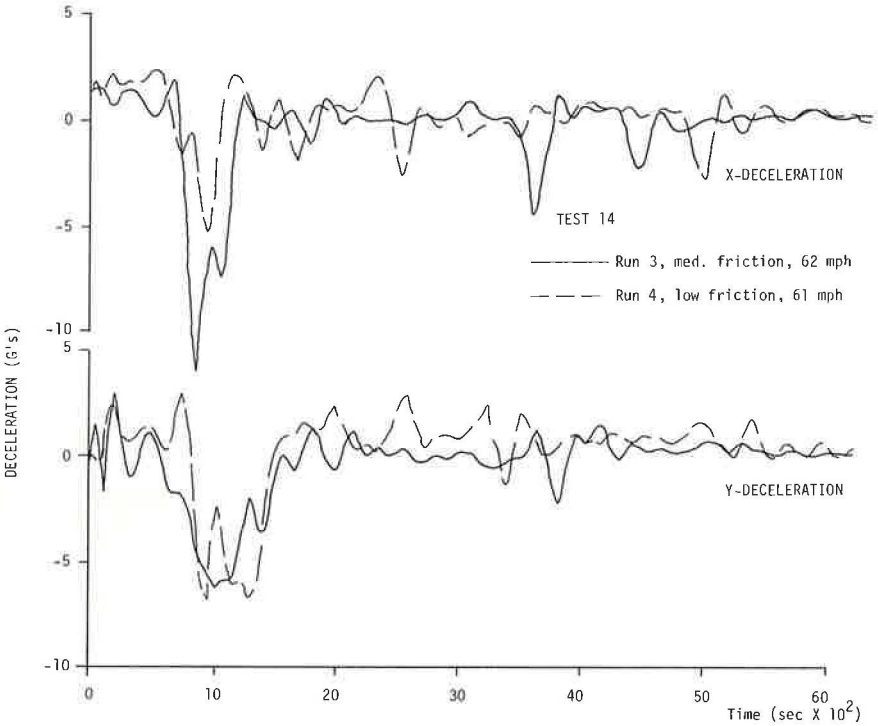

Table 3. Average pulse deceleration for medium- and low-friction tests.

Run No.[a]	Friction	Impact Speed (mph)	Average Pulse Deceleration[b] (*g*) Axial (X)	Lateral (Y)
1	Medium	61	4.97	1.96
2	Medium	62	4.00	3.08
3	Medium	62	5.46	2.60
4	Low	61	2.10	3.35
5	Low	61	2.81	3.06
6	Low	59	1.60	3.85

Note: 1 mph = 1.6 km/h.

[a]Test 14.

[b]Mean deceleration during period of pulse with 2-*g* cut-off level.

influence of the frictional forces at the vehicle-barrier interface is important. High-friction coefficients (μ = 1.35) are catastrophic in their effect, and low-friction coefficients (μ = 0.10) significantly reduce axial deceleration levels below those for medium-friction coefficients (μ = 0.85).

The influence of these factors for velocities ranging from 47 to 62 mph (76 to 100 km) has been investigated. The influence of the stiffness of the barrier structure has not been evaluated, but the influence of friction is believed to have more effect on lower stiffness structures because of the increased pocketing potential. Results of full-scale tests on concrete median barriers smeared with grease indicated no apparent difference in performance as compared with ungreased median barriers (16, 17). However, low-friction coefficients are not likely to be obtained in this manner since fluid pressures in the grease cannot be maintained unless adequate contact area can be developed to contain the fluid pressures. Deforming vehicle surfaces would most probably pierce the lubrication film.

This study implies that redirecting appurtenances should be designed for low values of vehicle interface-surface friction.

ACKNOWLEDGMENTS

This study was conducted at Brigham Young University. It was part of the development of high-performance crash barriers being conducted by Eyring Research Institute. The support of the Federal Highway Administration, U.S. Department of Transportation is gratefully acknowledged.

REFERENCES

1. Federal Motor Vehicle Safety Standards and Regulations, With Amendments and Interpretations Issued Through July 1974. National Highway Traffic Safety Administration, Standard 215, Aug. 1974.
2. Proposal for 45-50 mph Frontal Crashworthiness by Early 1980's. National Highway Traffic Safety Administration, Docket 74-14, Notice 1, March 19, 1974.
3. C. Y. Warner and D. Friedman. Automobiles and Highway Crash Attenuators: System Design Considerations. Transportation Research Record 488, 1974, pp. 19-23.
4. J. D. Michie and M. E. Bronstad. Location, Selection, and Maintenance of Highway Traffic Barriers. NCHRP Rept. 118, 1971.
5. J. L. Beaton and R. N. Field. Dynamic Full-Scale Tests of Median Barriers. HRB Bulletin 266, 1960, pp. 78-125.
6. B. S. Holmes and G. Sliter. Scale Modeling of Vehicle Crashes—Techniques, Applicability, and Accuracy; Cost Effectiveness. SAE, 3rd National Conference on Occupant Protection, Troy, Mich., Paper 740586, 1974.
7. B. S. Holmes and J. D. Colton. Scale Model Experiments for Safety Car Development. Trans., SAE, Paper 730073, 1973.
8. R. J. Fay and M. A. Kaplan. Energy-Absorbing Corrugated Metal Highway Buffer. Highway Research Record 460, 1973, pp. 20-29.
9. R. J. Fay and E. P. Wittrock. Scale-Model Test of an Energy-Absorbing Barrier. Highway Research Record 343, 1971, pp. 75-82.
10. R. I. Emori. Scale Model of Auto Collision With Breakaway Obstacles. Experimental Mechanics, Vol. 13, No. 2, Feb. 1973.
11. R. I. Emori. Scale Model Study Vehicle Collision Into Fixed Objects. Univ. of California, Los Angeles, Rept. UCLA-ENG-7106, Jan. 1971.
12. R. I. Emori. Analytical Approach to Automobile Collisions. SAE Annual Meeting, Detroit, Paper 680016, Jan. 1968.
13. M. P. Jurkat and J. A. Starrett. Automobile-Barrier Impact Studies Using Scale Model Vehicles. Highway Research Record 174, pp. 30-41.
14. H. L. Langhaar. Dimensional Analysis and Theory of Models. John Wiley, New York, 1951.
15. G. Murphy. Similitude and Engineering. Ronald Press, New York, 1950.
16. L. C. Lundstrom, P. C. Skeels, B. R. Englund, and R. A. Rogers. A Bridge Parapet Designed for Safety? General Motors Proving Ground Circular Test Track Project. Highway Research Record 83, 1965, pp. 169-187.
17. J. S. Starrett and I. R. Ehrlich. Highway Center-Barrier Investigation—Part 2. Davidson Laboratory, Stephens Institute of Technology, Rept. 1139, June 1967.
18. E. F. Nordlin et al. Dynamic Tests of a Prestressed Concrete Median Barrier Type 50, Series XXVI. State of California, Research Rept. CA HY MR 6588-1-73-06, March 1973.